

Soft Quantum Control for Highly Selective Interactions among Joint Quantum Systems

J. F. Haase, Z.-Y. Wang,* J. Casanova, and M. B. Plenio[†]

Institut für Theoretische Physik und IQST, Albert-Einstein-Allee 11, Universität Ulm, D-89069 Ulm, Germany

We propose a quantum control scheme aimed at interacting systems that gives rise to highly selective coupling among their near-to-resonance constituents. Our protocol implements temporal control of the interaction strength, switching it on and off again adiabatically. This soft temporal modulation significantly suppresses off-resonant contributions in the interactions. Among the applications of our method we show that it allows us to perform an efficient rotating-wave approximation in a wide parameter regime, the elimination of side peaks in quantum sensing experiments, and selective high-fidelity entanglement gates on nuclear spins with close frequencies. We apply our theory to nitrogen-vacancy centers in diamond and demonstrate the possibility for the detection of weak electron-nuclear coupling under the presence of strong perturbations.

Introduction.— The ability to selectively manipulate and couple the constituents in an interacting quantum cluster is a fundamental requirement for a wide range of technological applications [1–3]. For instance, the *individual addressing* of magnetic nuclei in a target molecule with a quantum sensor, such as the nitrogen-vacancy (NV) center in diamond [4], is a crucial requirement to determine the 3D structure of single molecules of interest for biochemistry and medicine [5–12]. In addition, the selective coupling of the quantum sensor with nearby quantum registers would enhance the sensitivity and resolution of quantum sensing protocols [13–18]. From a different point of view, if the addressing operation does not disturb the other qubits surrounding a certain target register, namely the ^{13}C and ^{29}Si nuclear spins that appear in diamond [19–23] and silicon carbide [24, 25], or Eu^{3+} ions in stoichiometric rare-earth crystals [26, 27], one can use the available qubits for quantum information [28–30] or quantum simulation [31] tasks. Furthermore, nuclear qubits coupled to an electron spin are also important to build a robust optical interface for quantum networks [32, 33].

The addressability problem can be reduced to the situation shown in Fig. 1 (a) where a control qubit (CQ) interacts with multiple resource qubits (RQs) [34, 35]. In order to exert control on a certain RQ the characteristic frequency ω_0 of the CQ is tuned to the resonance frequency ω_j of the RQ via a continuous drive that exploits the Hartmann-Hahn resonance [36–38] or the application of pulsed dynamical decoupling (DD) [39–43]. As we will show later, because of the time independent coupling c_j between the CQ and each RQ, the spectral responses are proportional to $c_j/\delta_{0,j}$ which decays slowly with the energy mismatch $\delta_{0,j} = \omega_0 - \omega_j$ ($j > 0$ for RQs), i.e. in a power-law manner. Therefore other off-resonant RQs will considerably perturb the CQ and vice versa, see Fig. 1 (b), prohibiting the high-fidelity addressing on the desired target RQ. This is particularly challenging for realistic settings where the RQs only slightly differ in their resonance frequencies.

In this Letter we propose the idea of soft temporal quantum control which enables on-resonant coupling within a desired set of target systems, while efficiently avoiding unwanted off-resonant contributions coming from others. With the specific case of Gaussian soft control, off-resonant effects are expo-

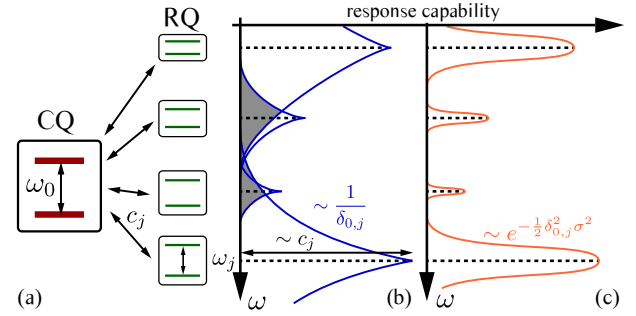


FIG. 1. Advantages of temporal shaping of coupling. (a) Illustration for the control qubit and resource qubits. (b) For the case of constant coupling c_j , the off-resonant response decays slowly $c_j/\delta_{0,j}$ (blue lines) with the energy mismatch $\delta_{0,j}$. The overlaps (gray areas) on the frequency response prohibit high-fidelity selective coupling. (c) With the soft coupling proposed in this work the off-resonant response decays exponentially (see the orange lines), which allows high-fidelity addressing.

ponentially suppressed by the mismatch $\delta_{0,j}$ as $\exp(-\sigma^2\delta_{0,j}^2/2)$, see Fig. 1 (c), achieving high-selective coupling. In addition, we develop an average Hamiltonian theory for our soft quantum control method. By using the quantum adiabatic theorem, we take high-order virtual transitions into account and provide an accurate description of the dynamics even for situations involving strong perturbations and long evolution times. We will show specific applications of our method such as the realization of an efficient rotating-wave approximation (RWA) and highly selective two-qubit gates for quantum sensing and computing.

Generic model.— To explore the effects emerging from temporal control, we consider the Hamiltonian ($\hbar = 1$) $H = H_S + H_{\text{int}}$, where H_S is the Hamiltonian for the quantum registers and $H_{\text{int}} = \lambda(t) \sum_{\alpha} c_{\alpha} V_{\alpha}$ describes their interactions that we want to perform selective control. $\lambda(t)$ is a dimensionless, time-dependent global factor and V_{α} may be single-body or N -body operators with strength c_{α} (i.e. the norm of V_{α} is bounded to one).

In terms of the eigenvalues ω_j and the projection operators

$\mathbb{P}(\omega_j)$ of the Hamiltonian $H_S = \sum_j \omega_j \mathbb{P}(\omega_j)$, we write

$$H_{\text{int}} = \lambda(t) \sum_{\alpha, j, k} c_\alpha V_\alpha^{\omega_j, \omega_k}, \quad (1)$$

where each $V_\alpha^{\omega_j, \omega_k} \equiv \mathbb{P}(\omega_j) V_\alpha \mathbb{P}(\omega_k)$ fulfils

$$[H_S, V_\alpha^{\omega_j, \omega_k}] = (\omega_j - \omega_k) V_\alpha^{\omega_j, \omega_k}. \quad (2)$$

In coupled quantum networks, $V_\alpha^{\omega_j, \omega_k}$ would describe the interaction between quantum systems with an energy mismatch of $\delta_{j,k} \equiv \omega_j - \omega_k$. Our target is to suppress the terms $V_\alpha^{\omega_j, \omega_k}$ in Eq. (1) for which $\omega_j \neq \omega_k$, and to keep the energy conserving ones (i.e. those with $\delta_{j,k} = 0$) by shaping the parameter $\lambda(t)$ for the sake of enhanced selectivity.

Leading-order effects and soft quantum control.— In a rotating frame with respect to H_S , H_{int} becomes $H'_{\text{int}}(t) = \lambda(t) \sum_{\alpha, j, k} c_\alpha V_\alpha^{\omega_j, \omega_k} e^{i\delta_{j,k}t}$. In the absence of a modulation for λ , i.e. $\lambda(t) = \lambda_0$, unwanted terms in V_α can be neglected by the RWA provided that the $\delta_{j,k}$ is sufficiently large compared with $\lambda_0 c_\alpha$. To see how the modulation of $\lambda(t)$ improves this situation, we calculate the leading-order effective Hamiltonian in the rotating frame by using the Magnus expansion [44, 45] for a time interval $[-T/2, T/2]$; it reads

$$\bar{H}_{\text{int}}^{(1)} = \frac{1}{T} \int_{-T/2}^{T/2} dt H'_{\text{int}}(t) = \sum_{\alpha, j, k} c_\alpha g(\delta_{j,k}) V_\alpha^{\omega_j, \omega_k}, \quad (3)$$

where the averaging factor

$$g(\delta_{j,k}) = \frac{1}{T} \int_{-T/2}^{T/2} dt \lambda(t) e^{i\delta_{j,k}t} \quad (4)$$

can be controlled by $\lambda(t)$.

For the conventional case of a constant $\lambda(t) = \lambda_0$, we have

$$g(\delta_{j,k}) = g_C(\delta_{j,k}) \equiv \lambda_0 \frac{\sin(T\delta_{j,k}/2)}{(T\delta_{j,k}/2)}. \quad (5)$$

In this manner, unwanted terms in V_α are suppressed by a large energy mismatch $\delta_{j,k}$ to decrease the value of $g_C(\delta_{j,k})$ [46]. By selecting λ_0 sufficiently small, the off-resonant interactions can be more efficiently suppressed with the associated improvement in the addressing for the resonant terms. See Refs. [9, 47] for a specific application of the latter to the case of NV centers in diamond surrounded by ^{13}C nuclear spins. However, from Eqs. (3) and (5) the effects introduced by off-resonant terms decay slowly as a power law $\lambda_0 c_\alpha / \delta_{j,k}$ on the energy mismatch $\delta_{j,k}$ while, in addition, because $g(0) = \lambda_0$ a decrease on λ_0 also carries the undesired effect of reducing the intensity of the coupling with the resonant terms.

From Eq. (4), we find that by using a time-dependent soft modulation, i.e., $\lambda(t)$ is small at the beginning and at the end of quantum evolution, the non-resonant terms can be removed with greater fidelity. More specifically, we propose the Gaussian temporal modulation

$$\lambda(t) = \lambda_0 \exp[-t^2/(2\sigma^2)], \quad (6)$$

which has the corresponding factor

$$g(\delta_{j,k}) = g_M(\delta_{j,k}) \equiv \lambda_0 \eta(\sigma, T) \exp\left(-\frac{1}{2}\sigma^2 \delta_{j,k}^2\right), \quad (7)$$

where $\eta(\sigma, T) = \frac{\sqrt{\pi}\sigma}{T} \left[\text{erf}\left(\frac{T-2i\sigma^2\delta_{j,k}}{2\sqrt{2}\sigma}\right) + \text{erf}\left(\frac{T+2i\sigma^2\delta_{j,k}}{2\sqrt{2}\sigma}\right) \right]$ and $\text{erf}(x) = \frac{2}{\sqrt{\pi}} \int_0^x dz e^{-z^2}$. A simple inspection of Eq. (7) reveals that the effective couplings $g_M(\delta_{j,k})c_\alpha$ decay exponentially with $\delta_{j,k}$. Hence, we expect the selectivity to be dramatically improved. We want to remark that our temporal shaping scheme shares interesting similarities with the control by Gaussian pulses of classical fields [48], however, in our case, the shaping is exerted on the coupling between quantum systems where quantum backaction plays a significant role on both sides [49].

Higher-order effects and adiabatic average Hamiltonian.— Although the leading-order average Hamiltonian $\bar{H}_{\text{int}}^{(1)}$ in Eq. (3) describes well the dynamics for $T \ll 1/\max|c_\alpha|$, if strong coupling constants are present, higher-order corrections [44, 45] have to be included in order to have an accurate description of the dynamics for larger times.

While the evaluation of higher-order terms is involved in the general case, now we will show that our proposed soft quantum control scheme allows us to easily describe the system propagator including high-order corrections when executed in an adiabatic manner. To this end we first analyze the propagator $U_D = \exp\left(-i \int_{-T/2}^{T/2} H_D dt\right)$, where $H_D = H_S + \lambda(t) \sum_\alpha c_\alpha \sum_j V_\alpha^{\omega_j, \omega_j}$ includes the on-resonance desired interactions. In the latter all $V_\alpha^{\omega_j, \omega_j}$ operators commute with H_S , see Eq. (2), hence H_D can be diagonalized in the common eigenstates $|\psi_n^D\rangle$ ($n = 1, 2, \dots$) of H_S and $V_\alpha^{\omega_j, \omega_j}$. Therefore $U_D = \sum_n e^{-i\phi_n^D(T)} |\psi_n^D\rangle \langle \psi_n^D|$ is also diagonal in the basis $\{|\psi_n^D\rangle\}$ and the dynamic phases $\phi_n^D(T)$ include the effect of energy shifts coming from $V_\alpha^{\omega_j, \omega_j}$.

If the whole Hamiltonian H is considered, the time-ordered evolution $U = \mathcal{T} \exp\left[-i \int_{-T/2}^{T/2} H(t) dt\right]$ is generally non-diagonal in the basis $\{|\psi_n^D\rangle\}$ and the non-commuting $V_\alpha^{\omega_j, \omega_k}$ terms would cause unwanted transitions between the different $|\psi_n^D\rangle$ states.

However, when the soft control is included one can efficiently eliminate the unwanted interactions caused by $V_\alpha^{\omega_j, \omega_k}$, even for long evolution times T . At the boundaries of the interaction times ($-T/2$ and $T/2$), $\lambda(t)$ has negligible values and therefore the system's eigenstates coincide with those of H_D . More precisely, under the condition of adiabatic evolution [50, 51], there are no transitions among the states $|\psi_n^D\rangle$ and the propagator at the end of the evolution is $U \approx \sum_n e^{-i\phi_n(T)} |\psi_n^D\rangle \langle \psi_n^D| \equiv \bar{U} \equiv e^{-i\bar{H}T}$, where $\phi_n(T)$ are the dynamic phases, while the geometric phases vanish because $\lambda(t)$ returns to its original value [52]. In this manner U takes the same form as U_D and the adiabatic average Hamiltonian for the soft quantum control scheme

$$\bar{H} = \sum_n [\phi_n(T)/T] |\psi_n^D\rangle \langle \psi_n^D|, \quad (8)$$

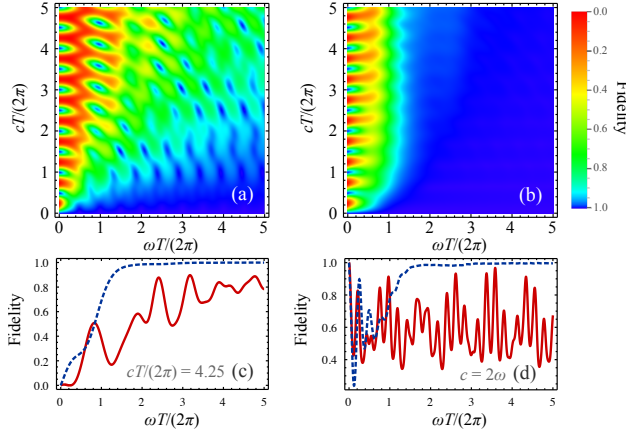


FIG. 2. (Color online) Fidelities under RWA. (a) Fidelity to the target evolution without unwanted coupling by using the constant-amplitude coupling. (b) As in (a) but using a Gaussian soft coupling with $\sigma = T/(4\sqrt{2})$ and $1/\lambda_0 = \sqrt{2\pi}\sigma \operatorname{erf}\left(\frac{T}{2\sqrt{2}\sigma}\right)$ such that we obtain the same target evolution. Curves in (c) and (d) show cross-sectional plots in the constant-amplitude case of (a) [red solid lines], or for the Gaussian shaped coupling case of (b) [blue dashed lines]. It is easy to see that the soft quantum control scheme keeps a high fidelity even for a relatively large ratios c/ω at long evolution times T .

is diagonal in the same basis as H_D and includes all the high-order energy shifts. In the following we illustrate our general theory via two important applications.

Improved RWA.— Here we demonstrate how the soft quantum control mechanism efficiently eliminates the non-energy-conserving (or counter rotating) terms over a continuous time interval even for long evolution times. The existence of the non-energy-conserving terms is due to the limit of available resources for selective control on realistic quantum systems (e.g., singlet-triplet qubits in semiconductor quantum dots [53, 54]). As an example, we consider a control qubit (0) and two equally strong coupled resource qubits (1, 2) (e.g., singlet-triplet qubits [53, 54]) with the interaction

$$H_{\text{int}} = c\lambda(t)\sigma_0^x(\sigma_1^x + \sigma_2^x) = c\lambda(t)(P_{0,1} + Q_{0,1} + \sigma_0^x\sigma_2^x), \quad (9)$$

where σ_j^α ($\alpha = x, y, z$) denotes a Pauli operator for the j -th qubit, $P_{0,1} = \sigma_0^+\sigma_1^- + \text{H.c.}$ with $2\sigma_j^\pm = \sigma_j^x \pm i\sigma_j^y$, and $Q_{0,1} = \sigma_0^+\sigma_1^+ + \sigma_0^-\sigma_1^-$. The coexistence of $P_{0,1}$ and $Q_{0,1}$ can be due to the nature of systems (see [54] for a realistic example). We aim to interact qubit 0 purely with qubit 1 via the flip-flop term $P_{0,1}$ without involving the perturbation $Q_{0,1}$. Therefore the energies $H_S = \frac{\omega}{2}(\sigma_0^z + \sigma_1^z) + \frac{\omega_2}{2}\sigma_2^z$ are chosen such that qubit 2 is off resonant with $\omega_2 = 3\omega$. The corresponding target Hamiltonian

$$H_{\text{target}} = \frac{1}{2}\tilde{\omega}(\sigma_0^z + \sigma_1^z) + \frac{1}{2}\tilde{\omega}_2\sigma_2^z + \tilde{c}(\sigma_0^+\sigma_1^- + \text{H.c.}), \quad (10)$$

with the associated propagator $U_{\text{target}} = e^{-iH_{\text{target}}T}$ can be used to generate high-fidelity swap gate between qubits 0 and 1. The corrected energies and interaction marked with a tilde can be obtained by using the adiabatic average Hamiltonian according to Eq. (8).

In Fig. 2 (a) and with the red solid lines in (c) and (d), we show the gate fidelities $F = |\text{Tr}(U_{\text{target}}U^\dagger)|/|\text{Tr}(UU^\dagger)|$ [55] (here $U = \mathcal{T} e^{-i\int_{-T/2}^{T/2}(H_S+H_{\text{int}})dt}$) with respect to the target evolution U_{target} for the standard coupling $\lambda(t) = 1$, while in Fig. 2 (b) and with the blue dashed lines in (c) and (d) the fidelities are plotted for a situation involving the soft quantum modulation in Eq. (6). An inspection of these plots reveals that the soft coupling approach results in much higher fidelities in a wide range of parameters, even for strong coupling regimes ($c > \omega$) and a wide range of evolution times. In contrast, the standard approach does not achieve a high fidelity to the target Hamiltonian because an efficient elimination of the oscillating terms requires weak couplings and longer averaging periods. Naturally during these times, relaxation and decoherence processes will decrease the fidelity further. Furthermore, locating the points of high fidelity in the standard approach becomes increasingly difficult when more qubits are involved (cf. the two-qubit example in the Supplemental Material [56]).

Note that our approach is fundamentally different from adiabatic elimination [57, 58]. Adiabatic elimination is aimed at *coupling* certain target levels by a virtual transfer of excitations through other mediator states that are removed from the dynamics, thus generating an evolution in the *reduced* Hilbert space of the target states. Instead our objective is to efficiently *suppress* unwanted interaction terms in the Hamiltonian through a soft modulation of the coupling constants, without reducing the dimension of the whole Hamiltonian and without having to use other states as mediators. Hence our method allows us to switch off unwanted interactions among the qubits in a highly selective manner and to perform high-fidelity quantum gates as we will demonstrate later.

Selective qubit addressing.— The soft quantum control mechanism allows high-fidelity interactions between weakly coupled qubits while it avoids perturbations that arise from the presence of strongly coupled qubits. Since the NV center in diamond is an excellent platform for quantum information processing [28–30], quantum networks [32, 33] and quantum sensing [5, 6], we consider a network consisting of an NV electron spin and its surrounding ^{13}C nuclear spins (see [56] for details of the model).

The electron-nuclear hyperfine coupling offers a medium to control the ^{13}C nuclear spins via the NV electron. Under pulsed DD [41–43, 47] or a continuous drive [37, 38] on the NV electron states $m_s = 0$ and, say, $m_s = -1$, the ^{13}C Larmor frequencies ω_j are shifted by hyperfine coupling, providing the frequency differences $\delta_{j,n} = \omega_j - \omega_n$ for selective addressing [56]. However, the differences $\delta_{j,n}$ and the electron-nuclear interactions are typically of the same order of magnitude, imposing a challenge on highly selective coupling.

To demonstrate the advantages of the soft quantum control, we compare different protocols in Fig. 3 by using a model with two spectrally close nuclear spins (their coupling is small but is taken into account in simulations). As shown in Fig. 3 (a) a frequency scan obtained via a continuous, constant drive [37, 38] does not resolve the two ^{13}C nuclei even for a

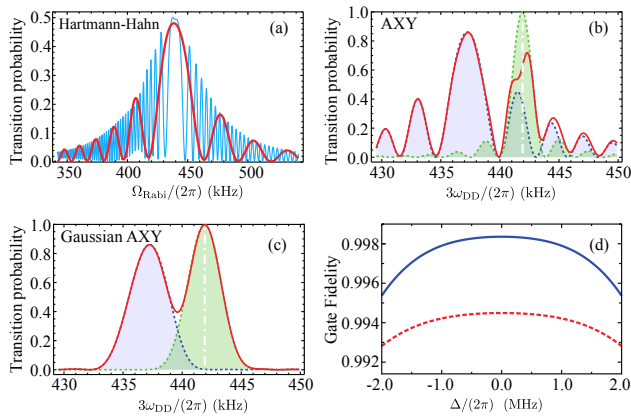


FIG. 3. (Color online) (a)-(c) Signal of transition probabilities, originating from two nuclear spins ($\omega_1 = 2\pi \times 441.91$ kHz and $\omega_2 = 2\pi \times 437.54$ kHz, see [56] for more details). (a) Hartmann-Hahn resonance spectrum with a total sensing time $T \approx 54 \mu\text{s}$ (red) or $T \approx 435 \mu\text{s}$ (blue). (b) Signal for AXY sequences (red solid line) at the third harmonic with 128 composite pulses each with five elementary π pulses. The single-spin contributions are drawn with dashed lines and corresponding shading, and $f_3 = 0.271$ is chosen to maximize the one from the first spin. The target signal centered at the vertical dash-dotted line is destroyed by the strong perturbation from the unwanted second spin. (c) Varying f_3 of the AXY sequences in (b) according to the Gaussian shape clearly resolves the two spins. (d) The fidelity (blue solid curve) of the gate $U_{\text{target}} = e^{-i\frac{\pi}{4}\sigma_0^z\sigma_1^x} \otimes \mathbb{I}_2$ as a function of the microwave detuning error Δ by using the Gaussian AXY sequence with a Rabi frequency $\Omega = 2\pi \times 20$ MHz in the rectangular pulses. The red dashed line is the case for a mismatch of 5% in Ω . To realize the gate U_{target} , f_3 has been reduced by a factor of two when using the parameters indicated by the vertical dashed-dotted line in (c).

longer sensing time T because of the slow power-law-decay of the signal around the resonance position.

Because pulsed DD sequences can be implemented easily in current experimental setups and coherent control on NV electron and nuclear spins longer than one second has been experimentally implemented with over ten thousands of DD pulses [30], we apply a DD sequence to preserve the coherence of the NV electron qubit and to realize the Hamiltonian [56]

$$H = -\frac{1}{8}f_{\text{kDD}}\sigma_0^z \sum_{j>0} a_j^\perp \sigma_j^x - \sum_{j>0} \frac{1}{2}\delta_{j,n}\sigma_j^z, \quad (11)$$

for addressing the nuclear frequency ω_n . Both $\delta_{j,n}$ and a_j^\perp are determined by the hyperfine coupling at the nuclear locations.

The DD protocol of adaptive-XY (AXY) sequences [47] provides better performance [9, 47] over standard DD sequences [39, 40] because it has strong robustness against control errors and allows us to tune f_{kDD} in a desirable manner. As shown in Fig. 3(b), by using a smaller f_{kDD} more signal details are revealed. However, this approach also reduces the coupling to the target spins.

By changing f_{kDD} in the AXY sequences for every unit with four composite pulses, we implement the Gaussian soft mod-

ulation $\lambda(t)$ in a digitized manner while preserving the robustness of the sequences against experimental control errors (see [56] for details). The resulting Gaussian AXY significantly enhances and resolves the weak-spin signal by using the soft modulation to eliminate the strong unwanted perturbation [see Fig. 3(c)]. In addition, it removes all the side peaks around the spin resonances, which is of great advantage when fitting dense signals [22] and avoids false identification of the signal peaks, in particular at the presence of spurious resonances [59–61]. Furthermore, it allows robust, high-fidelity quantum gates on the desired nuclear qubits. We calculate the fidelity for the gate $U_{\text{target}} = \exp(-i\pi\sigma_0^z\sigma_1^x/4) \otimes \mathbb{I}_2$ for the same parameters as the spectrum given in Fig. 3(c), but choose f_3 such that the target spin only performs a half rotation. We include an energy shift of the strongly coupled nuclear spin equivalent to the first example above. The fidelity is shown in Fig. 3(d) for different values of possible pulse errors. It is always well above 99%. On the contrary, the fidelities achieved by the Hartmann-Hahn or AXY protocol under the same condition are very low (e.g., 57% for AXY) because of the poor spin addressing [see Fig. 3(a),(b)]. Note that the enhanced spectral resolution by the soft control can be used to improve the controllability of interacting spin clusters [7–9, 16, 30] and nuclear-spin decoherence-free subspace [29].

Conclusions.— We proposed the mechanism of soft quantum control which enables highly selective coupling between different on-resonance constituents of composite quantum systems. The method introduces a time-dependent modulation of the coupling constants in addition to the matching of resonance frequencies. This results in an exponentially improved suppression of off-resonant couplings. Furthermore, we establish an adiabatic average Hamiltonian theory to describe interacting systems even under the presence of strong coupling terms to undesired parts of the Hilbert space. We showed two direct applications of our protocol: an improved RWA and, when combined with DD techniques, the addressing of weakly coupled nuclear spins under the presence of strong perturbations, originating from impurities with close resonance frequencies. The method is of general applicability and can be useful for the coherent manipulations of quantum registers and spectroscopic challenges in a wide range of systems such as stoichiometric rare earth ion systems, spin defects, and single dopants in solids, as well as spin-boson systems.

Acknowledgements.— This work was supported by the ERC Synergy grant BioQ and the EU Projects EQUAM and DIADEMS. J. C. acknowledges Universität Ulm for a Forschungsbonus. We thank Mark Mitchison for his careful reading of the manuscript. J.F.H. and Z.-Y.W. contributed equally to this work.

* zhenyu3cn@gmail.com

† martin.plenio@uni-ulm.de

- [1] F. J. Heremans, C. G. Yale, and D. D. Awschalom, Proc. IEEE **104** 2009 (2016).
- [2] E. Prati and T. Shinada, *Single-Atom Nanoelectronics* (Pan Stanford, 2013).
- [3] X. Rong, D. Lu, X. Kong, J. Geng, Y. Wang, F. Shi, C.-K. Duan, and J. Du, Adv. Phys. X **2**, 125 (2017).
- [4] M. W. Doherty, N. B. Manson, P. Delaney, F. Jelezko, J. Wrachtrup, and L. C. L. Hollenberg, Phys. Rep. **528**, 1 (2013).
- [5] R. Schirhagl, K. Chang, M. Loretz, and C. L. Degen, Annu. Rev. Phys. Chem. **65**, 83 (2014).
- [6] Y. Wu, F. Jelezko, M. B. Plenio, and T. Weil, Angew. Chem. Int. Ed. **55**, 6586 (2016).
- [7] N. Zhao, J. L. Hu, S. W. Ho, J. T. K. Wan, and R.-B. Liu, Nat. Nanotechnol. **6**, 242 (2011).
- [8] F. Shi, X. Kong, P. Wang, F. Kong, N. Zhao, R.-B. Liu and J. Du, Nat. Phys. **10**, 21 (2014).
- [9] Z.-Y. Wang, J. F. Haase, J. Casanova, and M. B. Plenio, Phys. Rev. B **93**, 174104 (2016).
- [10] W.-L. Ma and R.-B. Liu, Phys. Rev. Applied **6**, 024019 (2016).
- [11] J. M. Boss, K. Chang, J. Armijo, K. Cujia, T. Roskopf, J. R. Maze, and C. L. Degen, Phys. Rev. Lett. **116**, 197601 (2016).
- [12] W.-L. Ma and R.-B. Liu, Phys. Rev. Applied **6**, 054012 (2016).
- [13] I. Lovchinsky, A. O. Sushkov, E. Urbach, N. P. de Leon, S. Choi, K. De Greve, R. Evans, R. Gertner, E. Bersin, C. Müller, L. McGuinness, F. Jelezko, R. L. Walsworth, H. Park, and M. D. Lukin, Science **351**, 836 (2016).
- [14] T. Unden, P. Balasubramanian, D. Louzon, Y. Vinkler, M. B. Plenio, M. Markham, D. Twitchen, A. Stacey, I. Lovchinsky, A. O. Sushkov, M. D. Lukin, A. Retzker, B. Naydenov, L. P. McGuinness, and F. Jelezko, Phys. Rev. Lett. **116**, 230502 (2016).
- [15] S. Zaiser, T. Rendler, I. Jakobi, T. Wolf, S.-Y. Lee, S. Wagner, V. Bergholm, T. Schulte-Herbrüggen, P. Neumann, and J. Wrachtrup, Nat. Commun. **7**, 12279 (2016).
- [16] Z.-Y. Wang, J. Casanova, and M. B. Plenio, Nat. Commun. **8**, 14660 (2017).
- [17] Y. Matsuzaki, T. Shimo-Oka, H. Tanaka, Y. Tokura, K. Semba, and N. Mizuochi, Phys. Rev. A **94**, 052330 (2016).
- [18] T. Roskopf, J. Zopes, J. M. Boss, and C. L. Degen, npj Quantum Inf. **3**, 33 (2017).
- [19] G.-Q. Liu, H. C. Po, J. Du, R.-B. Liu, and X.-Y. Pan, Nat. Commun. **4**, 2254 (2013).
- [20] T. H. Taminiau, J. Cramer, T. van der Sar, V. V. Dobrovitski, and R. Hanson, Nat. Nanotechnol. **9**, 171 (2014).
- [21] G. Waldherr, Y. Wang, S. Zaiser, M. Jamali, T. Schulte-Herbrüggen, H. Abe, T. Ohshima, J. Isoya, J. F. Du, P. Neumann, and J. Wrachtrup, Nature (London) **506**, 204 (2014).
- [22] C. Müller *et al.* Nat. Commun. **5**, 4703 (2014).
- [23] V. V. Mkhitarian, F. Jelezko, and V. V. Dobrovitski, Sci. Rep. **5**, 15402 (2015).
- [24] P. G. Baranov, I. V. Il'in, E. N. Mokhov, M. V. Muzafarova, S. B. Orlinskii and J. Schmidt, JETP Lett. **82**, 441 (2005).
- [25] H. Seo, A. L. Falk, P. V. Klimov, K. C. Miao, G. Galli, and D. D. Awschalom, Nat. Commun. **7** 12935 (2016).
- [26] R. L. Ahlefeldt, W. D. Hutchison, and M. J. Sellars, J. Lumin. **130**, 1594 (2010).
- [27] R. L. Ahlefeldt, M. R. Hush, and M. J. Sellars, Phys. Rev. Lett. **117**, 250504 (2016).
- [28] J. Casanova, Z.-Y. Wang, and M. B. Plenio, Phys. Rev. Lett. **117**, 130502 (2016).
- [29] M. A. Perlin, Z.-Y. Wang, J. Casanova, and M. B. Plenio, arXiv:1708.09414.
- [30] M. H. Aboeib, J. Cramer, M. A. Bakker, N. Kalb, D. J. Twitchen, M. Markham, and T. H. Taminiau, arXiv:1801.01196.
- [31] J. Cai, A. Retzker, F. Jelezko, and M. B. Plenio, Nat. Phys. **9**, 168 (2013).
- [32] A. Reiserer, N. Kalb, M. S. Blok, K. J. M. van Bemmelen, T. H. Taminiau, R. Hanson, D. J. Twitchen, and M. Markham, Phys. Rev. X **6**, 021040 (2016).
- [33] N. Kalb, A. A. Reiserer, P. C. Humphreys, J. J. W. Bakermans, S. J. Kamerling, N. H. Nickerson, S. C. Benjamin, D. J. Twitchen, M. Markham, and R. Hanson, Science **356**, 928 (2017).
- [34] Q. Chen, I. Schwarz, and M.B. Plenio, Phys. Rev. Lett. **119**, 010801 (2017).
- [35] J. Casanova, Z.-Y. Wang, and M. B. Plenio, Phys. Rev. A **96**, 032314 (2017).
- [36] S. R. Hartmann, and E. L. Hahn, Phys. Rev. **128**, 2042 (1962).
- [37] J. Cai, F. Jelezko, M. B. Plenio, and A. Retzker, New J. Phys. **15**, 013020 (2013).
- [38] P. London, J. Scheuer, J.-M. Cai, I. Schwarz, A. Retzker, M. B. Plenio, M. Katagiri, T. Teraji, S. Koizumi, J. Isoya, R. Fischer, L. P. McGuinness, B. Naydenov, and F. Jelezko, Phys. Rev. Lett. **111**, 067601 (2013).
- [39] W. Yang, Z.-Y. Wang, and R.-B. Liu, Front. Phys. **6**, 2 (2011).
- [40] A. M. Souza, G. A. Alvarez, and D. Suter, Phil. Trans. R. Soc. A **370**, 4748 (2012).
- [41] S. Kolkowitz, Q. P. Unterreithmeier, S. D. Bennett, and M. D. Lukin, Phys. Rev. Lett. **109**, 137601 (2012).
- [42] T. H. Taminiau, J. J. T. Wagenaar, T. van der Sar, F. Jelezko, V. V. Dobrovitski, and R. Hanson, Phys. Rev. Lett. **109**, 137602 (2012).
- [43] N. Zhao, J. Honert, B. Schmidt, M. Klas, J. Isoya, M. Markham, D. Twitchen, F. Jelezko, R.-B. Liu, H. Fedder, and J. Wrachtrup, Nat. Nanotechnol. **7**, 657 (2012).
- [44] U. Haeberlen and J. S. Waugh, Phys. Rev. **175**, 453 (1968).
- [45] E. S. Mananga and T. Charpentier, Phys. Rep. **609**, 1 (2016).
- [46] Although the special matching condition $T\delta_{jk}/2 = n\pi$ ($n = 1, 2, \dots$) for $g(\delta_{jk}) = 0$ can be achieved for a single RQ with special values of the evolution time T , it is hard to accomplish for multiple RQs.
- [47] J. Casanova, Z. Y. Wang, J. F. Haase, and M. B. Plenio, Phys. Rev. A **92**, 042304 (2015).
- [48] L. M. K. Vandersypen, and I. L. Chuang, Rev. Mod. Phys. **76**, 1037 (2005).
- [49] N. Zhao, Z. Y. Wang, and R.-B. Liu, Phys. Rev. Lett. **106**, 217205 (2011).
- [50] Z.-Y. Wang and M. B. Plenio, Phys. Rev. A **93**, 052107 (2016).
- [51] K. Xu, T. Xie, F. Shi, Z.-Y. Wang, X. Xu, P. Wang, Y. Wang, M. B. Plenio, and J. Du, arXiv:1711.02911.
- [52] D. J. Griffiths, *Introduction to Quantum Mechanics*, 2nd ed. (Pearson Prentice-Hall, New Jersey, 2005).
- [53] M. P. Wardrop and A. C. Doherty, Phys. Rev. B **90**, 045418 (2014).
- [54] J. M. Nichol, L. A. Orona, S. P. Harvey, S. Fallahi, G. C. Gardner, M. J. Manfra, and A. Jacoby, npj Quantum Inf. **3**, 3 (2017).
- [55] X. Wang, C.-S. Yu, and X. X. Yi, Phys. Lett. A **373**, 58 (2008).
- [56] See Supplemental Material [url] for more details, which includes Refs. [62-64].
- [57] B. T. Torosov and N. V. Vitanov, J. Phys. B: At. Mol. Opt. Phys. **45**, 135502 (2012).
- [58] N. V. Vitanov, A. A. Rangelov, B. W. Shore, and K. Bergmann, Rev. Mod. Phys. **89**, 015006 (2017).
- [59] M. Loretz, J. M. Boss, T. Roskopf, H. J. Mamin, D. Rugar, and C. L. Degen, Phys. Rev. X **5**, 021009 (2015).
- [60] J. F. Haase, Z.-Y. Wang, J. Casanova, and M. B. Plenio, Phys. Rev. A **94**, 032322 (2016).

- [61] J. E. Lang, J. Casanova, Z.-Y. Wang, M. B. Plenio, and T. S. Monteiro, *Phys. Rev. Applied* **7**, 054009 (2017).
- [62] R. J. Epstein, F. M. Mendoza, Y. K. Kato, and D. D. Awschalom, *Nature Phys.* **1**, 94 (2005).
- [63] J. Zopes, K. Sasaki, K. S. Cujia, J. M. Boss, K. Chang, T. F. Segawa, K. M. Itoh, and C. L. Degen, *Phys. Rev. Lett.* **119**, 260501 (2017).
- [64] J.-M. Cai, B. Naydenov, R. Pfeiffer, L. P. McGuinness, K. D. Jahnke, F. Jelezko, M. B. Plenio, and A. Retzker, *New. J. Phys.* **14**, 113023 (2012).

Supplemental Material: Soft Quantum Control for Highly Selective Interactions among Joint Quantum Systems

I. EFFICIENT ROTATING-WAVE APPROXIMATION

A. Simplified example: two coupled qubits

To supplement the example given in the main text, we remove the second resource qubit of the model used in the main text (see the section titled ‘‘Improved RWA’’). This simplifies the illustration of the incapability of the standard approach to suppress the RWA terms efficiently. The total Hamiltonian becomes

$$H(t) = \frac{\omega}{2} (\sigma_0^z + \sigma_1^z) + c\lambda(t)\sigma_0^x\sigma_1^x. \quad (\text{S1})$$

As in the main text, we want to selectively preserve only the flip-flop interaction between the qubits. Explicitly, we would like to obtain the target Hamiltonian after RWA

$$H_{\text{target}} = \frac{1}{2}\tilde{\omega} (\sigma_0^z + \sigma_1^z) + \tilde{c}(\sigma_0^+\sigma_1^- + \text{H.c.}), \quad (\text{S2})$$

where the parameters take into account the energy shifts, as we explicitly show in the next section. In Fig. S1 the equivalent of Fig. 2 of the main text is shown. While the Gaussian modulation shows a smooth transition to constantly high fidelities, the standard method achieves high fidelity only for discrete values of ωT . Note that these discrete points for high fidelities in the standard method will change if there is a different number of qubits in the system (cf. Fig. 2 in the main text) and in general are hard to predict in complex systems.

B. Energy shifts

In the main text, we have shown that the soft quantum control scheme can efficiently eliminate oscillating terms while keeping desired energy-conserving interactions. Here we illustrate the calculation of energy shifts by considering the simple two-qubit Hamiltonian Eq. (S1) [with the target one given by Eq. (S2)]. To simplify the calculation, we first note that the subspaces $S_a = \{|\uparrow\uparrow\rangle, |\downarrow\downarrow\rangle\}$ and $S_b = \{|\uparrow\downarrow\rangle, |\downarrow\uparrow\rangle\}$ are disconnected in $H(t)$ by denoting as $|\uparrow\rangle$ ($|\downarrow\rangle$) the eigenstates of σ_j^z with the eigenvalues 1 (-1). In terms of the Pauli operators for the pseudo spin in each of the two subspaces, the Hamiltonian $H(t)$ can be written as

$$H(t) = \omega\sigma_a^z + c\lambda(t)\sigma_a^x + c\lambda(t)\sigma_b^x, \quad (\text{S3})$$

where $\sigma_a^z = |\uparrow\uparrow\rangle\langle\uparrow\uparrow| - |\downarrow\downarrow\rangle\langle\downarrow\downarrow|$ and $\sigma_a^x = |\uparrow\uparrow\rangle\langle\downarrow\downarrow| + \text{H.c.}$ are the Pauli operators in the subspace S_a and $\sigma_b^x = |\uparrow\downarrow\rangle\langle\downarrow\uparrow| + \text{H.c.}$ is the Pauli operator in the subspace S_b . Note that operators for different subspaces commute. The total field strength on the pseudo spin in the subspace S_a is

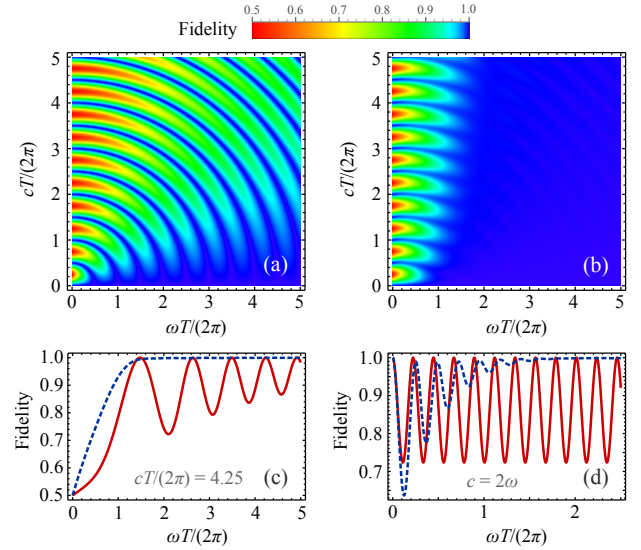


FIG. S1. (Color online) Fidelities to the target two-qubit dynamics. The figure is equivalent to Fig. 2 of the main text. The Gaussian shapes are realized with the parameters $\sigma = T/(4\sqrt{2})$ and $1/\lambda_0 = \sqrt{2\pi}\sigma\text{erf}\left(\frac{T}{2\sqrt{2}\sigma}\right)$ which ensures the same target evolution as in the constant amplitude case. (a) and (b) show the constant amplitude and Gaussian modulation respectively. The curves for the Gaussian shapes [blue dashed lines in (c) and (d)] illustrate the same characteristic asymptotic behavior as for the three qubit case, while the constant amplitude undergoes significantly less modulation as only a single frequency is left in the model.

$\sqrt{\omega^2 + c^2\lambda^2(t)}$ and the field strength for S_b is $c\lambda(t)$ which can be obtained by diagonalizing Eq. (S3). Similarly, we have

$$H_{\text{target}} = \tilde{\omega}\sigma_a^z + c\sigma_b^x, \quad (\text{S4})$$

with the corresponding field strengths of $\tilde{\omega}$ and $\tilde{c} = c$. For adiabatic modulation on $\lambda(t)$ (including the cases for $\lambda(t) = 1$ and soft coupling), the dynamic phases driven by $H(t)$ are the same as the case for H_{target} . As a consequence we obtain the energy

$$\tilde{\omega} = \frac{1}{T} \int_{-T/2}^{T/2} \sqrt{\omega^2 + c^2\lambda^2(t)} dt \quad (\text{S5})$$

by comparing the dynamic phase for the subspace S_a . The energy shifts $\tilde{\omega} - \omega$ include high-order effects in the average Hamiltonian theory. The dynamic phase for the subspace S_b is the average of the modulation $\frac{1}{T} \int_{-T/2}^{T/2} \lambda(t) dt = 1$.

II. ELECTRON-NUCLEAR SYSTEMS

A. Effective Hamiltonian

Consider the case of an NV electron spin coupled to its nearby nuclear spins. After the secular approximation that neglects the electron-spin flip terms, the Hamiltonian of this

system reads [S1–S3]

$$H_{\text{sys}} = DS_z^2 - \gamma_e B_z S_z - \sum_j \gamma_j B_z I_j^z + S_z \sum_j \vec{A}_j \cdot \vec{I}_j + H_{\text{n,n}}, \quad (\text{S6})$$

where S_z is the spin-1 operator of the NV electron spin projected on the NV symmetry axis (i.e., the z direction with the unit vector \hat{z}), $\vec{I}_j = \hat{x}I_j^x + \hat{y}I_j^y + \hat{z}I_j^z$ is the spin- $\frac{1}{2}$ operator for the j th nuclear spin, the zero-field splitting $D \approx 2\pi \times 2.87\text{GHz}$, B_z is the magnetic field applied along the \hat{z} direction, $\gamma_e \approx -2\pi \times 2.8\text{MHz/G}$ and γ_j are the gyromagnetic ratios of electron and ^{13}C nuclear spins respectively, \vec{A}_j describes the hyperfine interaction at the locations of the nuclear spins, and $H_{\text{n,n}}$ is the nuclear-nuclear dipolar coupling. For simplicity, the terms related to the nitrogen spin in the NV center have been neglected in the Hamiltonian H_{sys} , because their effects can be eliminated by dynamical decoupling (DD) [S2–S5] and (or) by the polarization of the nitrogen spin [S6]. We perform simulations according to the Hamiltonian H_{sys} .

We select two NV electron spin levels 0 and m_s ($m_s = +1$ or -1) to form the control qubit (with the Pauli operator $\sigma_0^z = |m_s\rangle\langle m_s| - |0\rangle\langle 0|$). For the simulations of robustness, the DD pulses are applied via the microwave field

$$H_{\text{ctr}} = \sqrt{2}\Omega \cos(\omega_{\text{mw}}t + \phi)S_x, \quad (\text{S7})$$

where Ω is the Rabi frequency of the rectangular pulses, ω_{mw} is the microwave frequency that are set to the frequency of the NV control qubit with a detuning $\Delta = \omega_{\text{mw}} - (D - m_s \gamma_e B_z)$, ϕ is an initial phase that control the effective directions of the DD pulses. In the rotating frame of the NV electron spin Hamiltonian $DS_z^2 - \gamma_e B_z S_z$, H_{ctr} realizes the driving

$$H_{\text{ctr}}^{\text{qubit}} = \frac{1}{2}\Omega[\sigma_0^x \cos(\phi) + \sigma_0^y \sin(\phi)], \quad (\text{S8})$$

on the control qubit with a Rabi frequency Ω . Here $\sigma_0^x = |m_s\rangle\langle 0| + |0\rangle\langle m_s|$.

In the following, we consider fast DD pulses that the exchange of the spin levels 0 and m_s (i.e., $\sigma_0^z \rightarrow -\sigma_0^z$) by each π pulse can be treated as instantaneously. Under the control of DD π pulse sequences, the relevant Hamiltonian in the rotating frame becomes [S2, S3]

$$H_{\text{e,n}} = \frac{m_s}{2}F(t)\sigma_0^z \sum_j \vec{I}_j \cdot \vec{A}_j - \sum_j \vec{I}_j \cdot \vec{\omega}_j, \quad (\text{S9})$$

where the vectors

$$\omega_j = \omega_j \hat{\omega}_j = \gamma_j B_z \hat{z} - \frac{1}{2}m_s \vec{A}_j \quad (\text{S10})$$

describe the nuclear precession frequencies (effective nuclear Zeeman energies) $\omega_j = |\vec{\omega}_j|$. The modulation function $F(t) = (-1)^{m(t)}$ when a number $m(t)$ of π pulses that has been applied until the time t . For homonuclear spin clusters such as the case of ^{13}C spins in diamond, the gyromagnetic ratios $\gamma_j \approx 2\pi \times 1.07\text{kHz/G}$ are identical, but ω_j are shifted by the hyperfine coupling at the locations of the nuclei. In the rotating frame

with respect to $-\omega_n \sum_j \vec{I}_j \cdot \hat{\omega}_j$, where ω_n is the target nuclear frequency to be addressed, the Hamiltonian becomes

$$H'_{\text{e,n}} = \frac{m_s}{2}F(t)\sigma_0^z \sum_j \vec{I}_j \cdot \vec{A}_j(t) - \sum_j \delta_{j,n} \vec{I}_j \cdot \hat{\omega}_j, \quad (\text{S11})$$

where $\delta_{j,n} = \omega_j - \omega_n$ are the frequency differences and

$$\vec{A}_j(t) = \vec{a}_j^x \cos(\omega_n t) + \vec{a}_j^y \sin(\omega_n t) + \vec{a}_j^z, \quad (\text{S12})$$

with $\vec{a}_j^x \equiv \vec{A}_j - \vec{a}_j^z$, $\vec{a}_j^y \equiv \hat{\omega}_j \times \vec{A}_j$, $\vec{a}_j^z \equiv a_j^{\parallel} \hat{\omega}_j$. The magnitudes $a_j^{\parallel} = \vec{A}_j \cdot \hat{\omega}_j$ and $|\vec{a}_j^x| = |\vec{a}_j^y| = a_j^{\perp}$. Because \vec{a}_j^{α} ($\alpha = x, y, z$) are in orthogonal directions, we denote the spin operators $I_j^{\alpha} = \vec{I}_j \cdot \vec{a}_j^{\alpha} / |\vec{a}_j^{\alpha}|$ and $I_j^{\pm} = I_j^x \pm iI_j^y$. Now we can write

$$H'_{\text{e,n}} = \frac{m_s}{4}F(t)\sigma_0^z \left[(a_j^{\perp} I_j^{\pm} e^{-i\omega_n t} + \text{h.c.}) + a_j^{\perp} I_j^z \right] - \sum_j \delta_{j,n} I_j^z. \quad (\text{S13})$$

We choose $F(t)$ to be symmetric and periodic $F(t + 2\pi/\omega_{\text{DD}}) = F(t)$, hence it can be represented by a Fourier series, $F(t) = \sum_k f_k \cos(k\omega_{\text{DD}}t)$ with the DD frequency ω_{DD} and $f_k = 0$ for even k . We tune the k_{DD} -th harmonic on resonance with the target nuclear frequency ω_n , i.e. $k_{\text{DD}}\omega_{\text{DD}} = \omega_n$. The nuclear spin frequencies $\omega_j \sim \gamma_j B_z$ can be made significantly larger than the hyperfine coupling in experiments by using a strong magnetic field. As a consequence, one can safely apply RWA to remove the counter-rotating terms in $H'_{\text{e,n}}$, which yields

$$H'_{\text{e,n}} = \frac{m_s}{4}f_{k_{\text{DD}}}\sigma_0^z \sum_j a_j^{\perp} I_j^x - \sum_j \delta_{j,n} I_j^z. \quad (\text{S14})$$

Under strong magnetic fields, $\hat{\omega}_j \approx \hat{z}$ is along the magnetic field direction. As a consequence, $a_j^{\parallel} \approx \vec{A}_j \cdot \hat{z}$ and a_j^{\perp} are the parallel and perpendicular components of \vec{A}_j with respect to the magnetic field $B_z \hat{z}$. The effective nuclear Larmor frequencies $\omega_j \approx \gamma_j B_z - \frac{1}{2}m_s a_j^{\parallel}$ and detunings $\delta_{j,n} \approx \frac{1}{2}m_s (a_j^{\parallel} - a_n^{\parallel})$ are determined by the hyperfine fields at the locations of nuclei.

For the case that $m_s = -1$ and ^{13}C spins in diamond $I_j^{\alpha} = \frac{1}{2}\sigma_j^{\alpha}$, the Hamiltonian $H'_{\text{e,n}}$ becomes the one of Eq. (11) in the main text

$$H = -\frac{1}{8}f_{k_{\text{DD}}}\sigma_0^z \sum_{j>0} a_j^{\perp} \sigma_j^x - \sum_{j>0} \frac{1}{2}\delta_{j,n} \sigma_j^z. \quad (\text{S15})$$

For CPMG or the XY family of sequences, ω_{DD} is fixed by the application of π pulses at times $t_p = \pi(p - 1/2)/\omega_{\text{DD}}$, $p = 1, 2, \dots$. However, a strategy like that yields constant Fourier coefficients f_k which are not tunable.

B. AXY sequences

The coupling coefficients f_k can be tuned via changing the pulse intervals. The AXY sequences employ robust composite pulses to tune $f_{k_{\text{DD}}}$ in a desirable way [S2]. As shown in

Fig. S2(a), each of the composite pulses consists of five elementary π pulses in a symmetric sequence, and the relative timing of the elementary π pulses determines the effective values of $f_{k_{\text{DD}}}$. In an AXY sequence [S2], the timing of each composite pulse is the same such that $f_{k_{\text{DD}}}$ has the same value though out the sequence.

C. Gaussian AXY sequences

The ability to continuously tune $f_{k_{\text{DD}}}$ by changing the relative timing of the elementary π pulses [see Fig. S2(a)] allows to simulate the modulation $\lambda(t)$ for soft quantum control. For the case that the change of $f_{k_{\text{DD}}}$ resembles a Gaussian shape [see Fig. S2(b)], we call the sequence Gaussian AXY sequences. In order to preserve the robustness of the sequences [S2], we only change $f_{k_{\text{DD}}}$ in the AXY-8 sequences for every unit with four composite pulses (XYXY or YXYX). In this manner, the first-order control errors are cancelled completely, while the second-order errors are small because of the symmetric XY-8 block (XYXYXYXY).

D. Hartmann-Hahn resonance

For the case of Hartmann-Hahn resonance, one can continuously drive the NV electron spin via the control Eq. (S7) for a sensing time T and scan the Rabi frequency $\Omega = \Omega_{\text{Rabi}}$ [S7, S8]. Under the continuous driving, we have the Hamiltonian for the relevant levels of the NV electron qubit,

$$H_{\text{H-H}} = H_{\text{ctr}}^{\text{qubit}} - \sum_j \gamma_j B_z I_j^z + m_s |m_s\rangle \langle m_s| \sum_j \vec{A}_j \cdot \vec{I}_j, \quad (\text{S16})$$

where $H_{\text{ctr}}^{\text{qubit}}$ is given by Eq. (S8) and we have neglected the weak nuclear-nuclear interaction $H_{\text{n,n}}$ for simplicity. $H_{\text{H-H}}$ is equivalent to

$$H'_{\text{H-H}} = \frac{\Omega_{\text{Rabi}}}{2} \sigma_0^x + \frac{m_s}{2} \sigma_0^z \sum_j \vec{A}_j \cdot \vec{I}_j - \sum_j \gamma_j B_z I_j^z + \frac{1}{2} \sum_j \vec{A}_j \cdot \vec{I}_j, \quad (\text{S17})$$

where for simplicity we have chosen $\phi = 0$ and $\Omega = \Omega_{\text{Rabi}}$ in $H_{\text{ctr}}^{\text{qubit}}$. One may define $\tilde{\sigma}_0^z = \sigma_0^x$ and $\tilde{\sigma}_0^x = \sigma_0^z$. By scanning the dressed-state energy Ω_{Rabi} to the the energies ω_j of nuclear spins, electron-nuclear flip-flop process is no longer suppressed by the energy mismatch and change the population of the electron qubit, resulting in signals in the spectrum [S7, S8].

E. Simulation details

In the simulations of the NV center, we use the system Hamiltonian Eq. (S6) that include electron-nuclear and nuclear-nuclear interactions. The effect of nuclear-nuclear interaction is negligible because it is weak compared with the

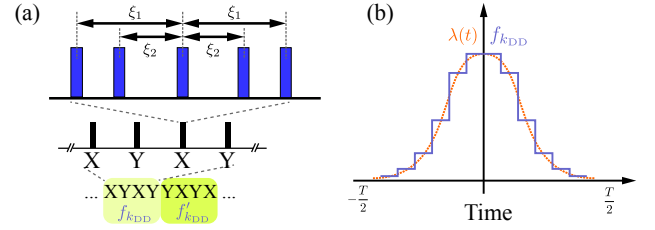


FIG. S2. (Color Online) Gaussian AXY sequence. (a) The upper part shows the symmetric configuration of an AXY composite pulse, where the relative times ξ_1 and ξ_2 among the elementary pulses determine the value of $f_{k_{\text{DD}}}$. The lower part shows that each four composite pulses build a robust XYXY or YXYX block of the same $f_{k_{\text{DD}}}$. Each block in the AXY sequence employs a different $f_{k_{\text{DD}}}$ for a soft modulation protocol in a manner that resembles the Gaussian shape as shown in (b). In the simulation for the results in the main text, we used the Gaussian shapes with $\sigma = T/(4\sqrt{2})$.

time scale of the simulations and the electron-nuclear coupling. To take into account the realistic situations that the control has detuning and amplitude errors, we use the control Hamiltonian Eq. (S7). We do not consider phase error in the control Eq. (S7) because it is negligibly small in typical NV experiments that use an arbitrary waveform generator [S9].

The NV electron spin is located at $(0, 0, 0)$ while the external magnetic field of $B_z = 400$ G is applied along the NV symmetry axis along the direction $(1, 1, 1)/\sqrt{3}$. In this basis, the two ^{13}C nuclei giving the resonance peaks in the main text are located at the diamond lattice sites $(0.26775, 0.62475, 0.80325)$ nm and $(0.80325, 0.08925, 0.08925)$ nm, with the corresponding $\omega_1 = 2\pi \times 441.91$ kHz, $\omega_2 = 2\pi \times 437.54$ kHz, $a_1^x = 2\pi \times 16.91$ kHz, and $a_2^x = 2\pi \times 54.26$ kHz. In sensing nuclear spins, we initialize the NV electron qubit to an eigenstate of σ_0^x and measure the change of the population on the initial state of the NV electron qubit [Fig. 3(a)-(c) in the main text]. In the simulation for the quantum gate [Fig. 3(d) in the main text], we take the shifted energies of the nuclear spins, similarly to Eq. (S5) into account. We would also like to point out that in the experiments on NV centers generally the fluctuation on the Rabi frequency (e.g., 2.4×10^{-3} in [S10]) is much smaller than the Rabi error (5%) which we used in the simulation of the main text. The detuning error Δ on the microwave field mainly originates from the unpolarized nitrogen nuclear spin intrinsic to the NV center [S11], and by polarizing the nitrogen spin the detuning error becomes negligible in the AXY sequences. Note that our simulated results are also valid when there is a large nuclear spin bath (e.g., without the use of an isotopically-purified diamond sample), because the DD sequences can efficiently suppressed the effect of other nuclear spins that have distinct frequencies than the frequency of the target nuclear spins. For example, using a DD sequence that has a lower spectral resolution and hence lower nuclear-spin addressability than the AXY and the soft Gaussian AXY sequences simulated in the main text, Ref. [S12] has already experimentally demonstrated selective addressing of 19 nuclear

spins in a diamond with a natural abundance (1.1%) of ^{13}C spins.

* zhenyu3cn@gmail.com

† martin.plenio@uni-ulm.de

- [S1] N. Zhao, J. L. Hu, S. W. Ho, J. T. K. Wan, and R.-B. Liu, *Nature Nanotechnol.* **6**, 242 (2011).
- [S2] J. Casanova, Z.-Y. Wang, J. F. Haase, and M. B. Plenio, *Phys. Rev. A* **92**, 042304 (2015).
- [S3] Z.-Y. Wang, J. F. Haase, J. Casanova, and M. B. Plenio, *Phys. Rev. B* **93**, 174104 (2016).
- [S4] W. Yang, Z.-Y. Wang, and R.-B. Liu, *Front. Phys.* **6**, 2 (2011).
- [S5] A. M. Souza, G. A. Álvarez, and D. Suter, *Phil. Trans. R. Soc. A* **370**, 4748 (2012).
- [S6] R. J. Epstein, F. M. Mendoza, Y. K. Kato, and D. D. Awschalom, *Nature Phys.* **1**, 94 (2005).
- [S7] J. Cai, F. Jelezko, M. B. Plenio, and A. Retzker, *New J. Phys.* **15**, 013020 (2013).
- [S8] P. London, J. Scheuer, J.-M. Cai, I. Schwarz, A. Retzker, M. B. Plenio, M. Katagiri, T. Teraji, S. Koizumi, J. Isoya, R. Fischer, L. P. McGuinness, B. Naydenov, and F. Jelezko, *Phys. Rev. Lett.* **111**, 067601 (2013).
- [S9] J. Zopes, K. Sasaki, K. S. Cujia, J. M. Boss, K. Chang, T. F. Segawa, K. M. Itoh, and C. L. Degen, *Phys. Rev. Lett.* **119**, 260501 (2017).
- [S10] J.-M. Cai, B. Naydenov, R. Pfeiffer, L. P. McGuinness, K. D. Jahnke, F. Jelezko, M. B. Plenio, and A. Retzker, *New J. Phys.* **14**, 113023 (2012).
- [S11] M. Loretz, J. M. Boss, T. Rosskopf, H. J. Mamin, D. Rugar, C. L. Degen, *Phys. Rev. X* **5**, 021009 (2015).
- [S12] M. H. Abobeih, J. Cramer, M. A. Bakker, N. Kalb, D. J. Twitchen, M. Markham, and T. H. Taminiau, arXiv:1801.01196.